Design of a Self-Recharging Untethered Mobile Inspection Tool inside a Pipeline

Wadie R. Chalgham[*1], and Abdennour C. Seibi[1]
[1]University of Louisiana at Lafayette
*P.O. Box 40029, Lafayette, LA 70504, wadie.chalgham@gmail.com

Abstract: Pipeline inspection tools present some limitations related to power supply which require recharging after each operation. Using batteries or tethered tools make the duration to inspect any pipeline very limited and time consuming. This paper aims at designing a spherical self-recharging untethered mobile ball flowing inside a given pipeline using COMSOL Multiphysics. The ball will be equipped with the necessary sensors to be able to detect any leaks through acoustic waves, and then send a signal to the supervisors once a leak was detected. The simulation described the energy gained by the rotation of the blades inside the ball. In addition, this paper presents a sensitivity analysis to optimize the number of openings and their location through the ball for maximum energy gain.

Keywords: Power Optimization, Fluid Flow, Pipeline Inspection, Efficiency, Environment

1. Introduction: Limitations of Existing Pipeline Inspection Technologies

Pipeline inspection tools and methods have advanced with time, using new available technologies and techniques. However, the commonly adopted inspection tools used to detect leaks in pipelines still present some limitations, such as high operation cost and low accuracy in detecting leak location. For instance, Smart Ball inspection tool, provided by Pure Technologies Ltd, has a low sensitivity since it is not capable of detecting leaks in pipelines that operate at pressures less than 10 psi and a low accuracy of leak location of ± 6 ft (± 2 m). This tool has a limited working range also because of the use of batteries, which makes it inconvenient for continuous real time data (Gernand and Ojala, 2011). Another commonly used inspection method is the use of tethered tools such as Sahara, provided by Pure Technologies Ltd, or LDS1000™, provided by JD7 Tech. These tools have limited survey lengths because of the tether cable and require numerous access points which make the use of this tool very expensive to operate. Ultrasonic Intelligent Pigging is another inspection technique that is limited to ferrous pipes only. It is not designed to differentiate between leaks and deep wall defects (Carlson and Henke, 2013). However, Acoustic Fiber Optic Monitoring (AFO) inspection technique presents very accurate results but at high operating costs. The installation and online monitoring costs are very significant with up to $64,000 per mile and up to $150,000 for hardware monitoring costs (Ariaratnam and Chandrasekaran, 2010). Moreover, the described tools and techniques are not autonomous and self-recharging, additional costs are associated with tools retrieval, additional man power and battery replacement. In addition, hard working conditions like rain or snow will prevent the working team from installing these tools; thereby, increasing the non-productivity time of these inspection tools.

2. Objectives and Scope

This preliminary study aims at developing a new inspection tool that consists of a ball capable of detecting leaks inside pipelines using acoustic signals. The ball is fully autonomous and does not need any change of battery using built-in blades, designed in COMSOL, which are installed inside the spherical ball. The blades are the driving components of the ball by using the force of the flow in order to rotate and generate a magnetic field that will induce a current. Thus, as long as the ball is propelled inside the pipeline by the fluid motion, the ball will be self-recharged. The simulation results of the fluid flow inside the ball presented the energy gain of incorporating the blades inside the spherical ball. Moreover, the sensitivity analysis compared the energy gain generated by multiple openings at various locations. This analysis aims at designing the most power efficient model of the flowing spherical ball.

3. Use of COMSOL Multiphysics® Software

COMSOL was first used to design the geometry of the spherical ball as well as its internal components including the rotating blades. Computational Fluid Dynamics (CFD) module was then used to simulate the fluid flow around the blades from which the associated energy to be used for charging the battery will be estimated. The battery self-charging rate will be determined from the obtained data. The results from the velocity propagation will be used to optimize the design of the outer shell of the ball by varying the number of openings. The optimal design is intended to generate enough power to recharge the batteries using the fluid flow. By having an autonomous power supply, this inspection tool will provide data in real time, improving the efficiency of this inspection tool.

4. Model Design

The geometry of the ball was created in COMSOL using the geometry builder feature. Figure 1 presents the design of the outer shell of the ball in the form of snapshots from different side views. It shows the spherical shape of the inspection tool as well as the multiple openings that allow the fluid to flow inside the ball. The top section of the ball incorporates the acoustic sensors and the lower section holds the battery, which will be self-recharged using the energy gained from the rotating blades caused by the fluid flow inside the ball. Figure 1 also shows that the openings are created at a direction perpendicular to the rotation axle direction to achieve a maximal rotational velocity of the blades. Figure 2 focuses on the design of the rotating blades. It shows four elliptic blades attached to the rotating axle. The two top blades have a different concave direction than the lower two blades, creating an S shape which is commonly used in renewable energy techniques. In fact, when the fluid flows inside the ball, the top two blades will be filled with fluid; whereas, the lower two blades having a concave down shape will resist the flow of the fluid, creating a mass difference which will induce an angular momentum, enabling the rotation of the blades in a clockwise direction.

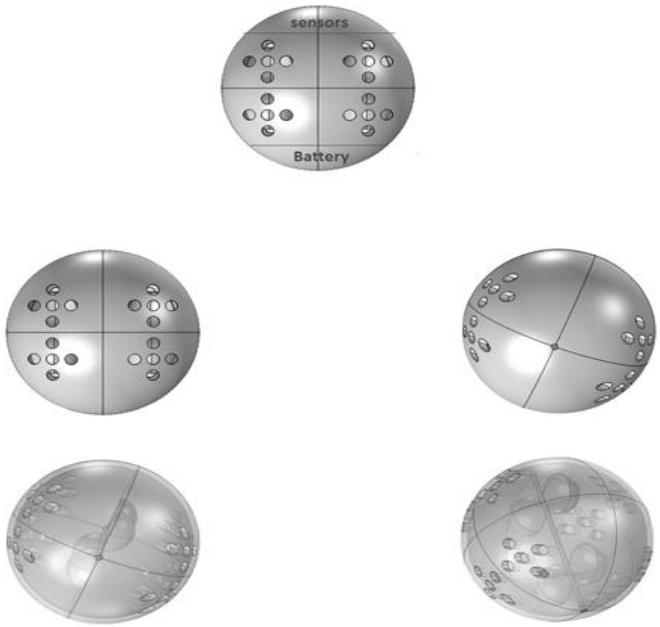

Figure 1. Design of the Ball Outer Shell

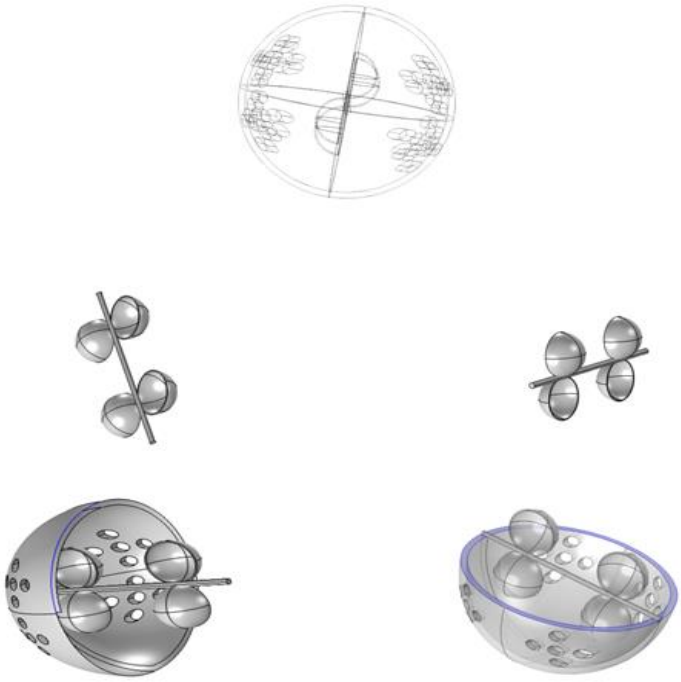

Figure 2. Design of the Rotating Blades

5. Simulation Results

5.1 Numerical Simulation of Velocity and Pressure Profiles without Openings

This simulation used the Computational Fluid Dynamics (CFD) module. The aim of the next two subsections is to show how the creation of openings in the ball generates energy by presenting the velocity and pressure profiles with and without openings. Water was used as the flowing fluid and pumped at an inlet velocity of 1 mm/s.

Figure 3 shows the velocity profile of the fluid flowing inside a pipe having a spherical ball with no openings. The simulation shows how the velocity magnitude of the fluid inside the pipe increases around the ball from the upper and lower directions. Figure 4 presents the related pressure magnitudes and shows a zero pressure inside the ball since it does not have any openings.

5.2 Numerical Simulation of Velocity and Pressure Profiles with Openings

In order to understand the effect of the created openings, two holes were placed at the top side of the ball as shown in Figure 5. The results show how the openings enabled the fluid flow inside the ball and how the velocity magnitude at the blade is no longer zero. The exact change in velocity is studied in more depth in the sensitivity section of this paper. Figure 6 presents the related pressure profiles and shows high pressure build up at the edge of the top blade with a maximum value of 2 mPa, confirming the effect of openings on the rotation of the blades, in a clockwise direction. The average velocity in sections 1 and 2 was estimated using the following equation:

$$\bar{v} = \frac{1}{L}\int_0^L v(x)\,dx \qquad (1)$$

The simulation results are used in the next sections to calculate the angular velocity ω of the shaft-blade system, from which the rotational kinetic energy (KE = ½ $I\,\omega^2$) was estimated.

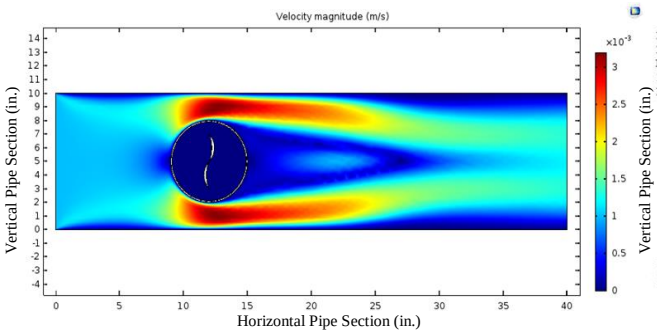

Figure 3. Velocity Propagation around the Ball without Openings

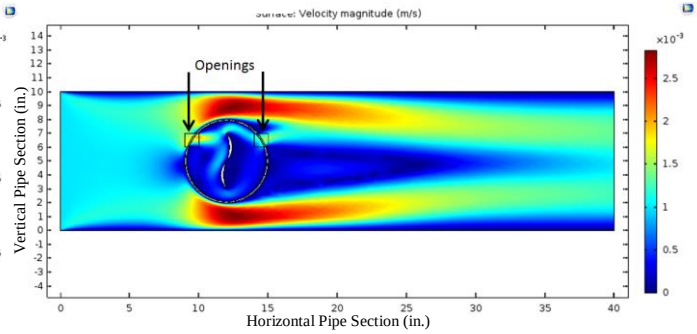

Figure 5. Velocity Propagation around the Ball with Openings Enabling the Rotation of the Blades

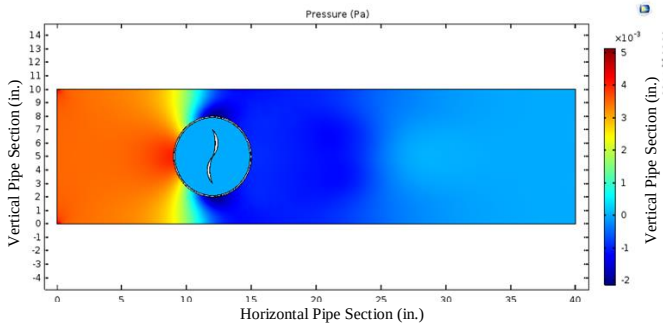

Figure 4. Pressure Propagation around the Ball without Opening

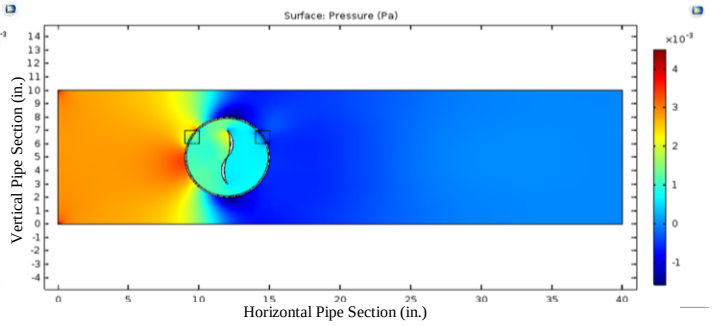

Figure 6. Pressure Propagation around the Ball with Openings Enabling the Rotation of the Blades

6. Sensitivity Analysis

The results presented so far are a special case of ball design where two openings were created. In order to optimize the design of the ball for a maximal energy gain, different opening numbers and locations should be varied to find the most efficient ball design.

Figure 7 presents the location of four openings: openings A and B are located at the upper side of the ball and openings C and D at the lower side.

Figure 8 shows two vertical sections having a length of 2 in. where the velocity magnitudes will be plotted. Section 1 is at the top side of the blade system while section 2 is at the lower side. The creation of these vertical sections aims at estimating the effective velocity of the shaft rotation, which is calculated by subtracting the values obtained along the vertical section 2 from the vertical section 1.

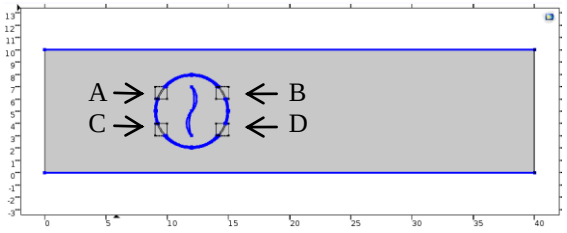

Figure 7. Four Openings Locations

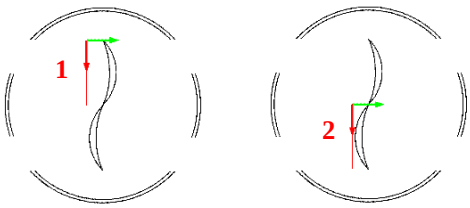

Figure 8. Location of Vertical Sections

6.1 Numerical Simulation of Velocity Profiles when using One Opening

To simulate the fluid flow inside the ball when using only one hole, opening A was opened whereas openings B, C and D were closed. Figure 9 shows the velocity propagation inside the pipe; while Figure 10 shows the velocity distribution at the selected vertical sections 1 and 2. The difference between the average velocity at section 1 and the average velocity at section 2 resulted in a magnitude of 0.023 mm/s indicating that having one opening doesn't increase significantly the fluid velocity magnitudes inside the ball.

This difference is very small and needs to be higher to generate enough velocity at and around the blades in order to provide rotational energy. As a result, the next sections will focus on the effect of multiple openings on the fluid flow velocity and blades rotation.

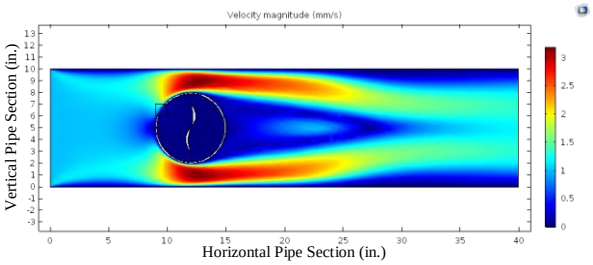

Figure 9. Velocity Propagation around and inside the Ball with One Opening

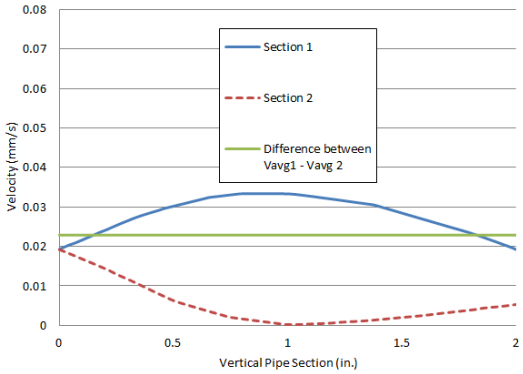

Figure 10. Fluid Velocity Magnitudes along Two Vertical Sections

6.2 Numerical Simulation of Velocity Profiles when using Two Openings

To simulate the fluid flow inside the ball when using two holes, different combinations were compared: openings A and B opened, openings A and D opened and openings A and C opened to fluid flow. Figures 11a, 11b and 11c show the velocity propagation inside the ball with two openings, A and B, A and D, and A and C respectively.

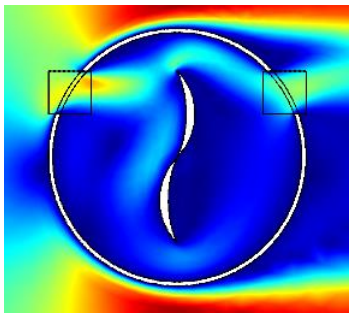

Figure 11a. Fluid Velocity Profile with Openings A and B

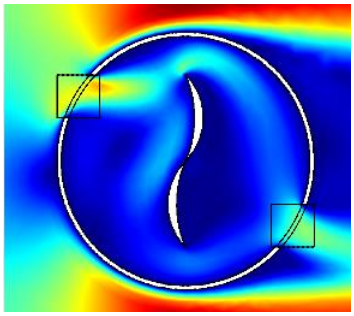

Figure 11b. Fluid Velocity Profile with Openings A and D

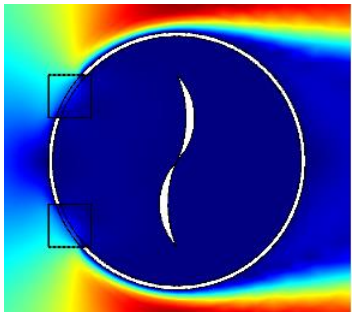

Figure 11c. Fluid Velocity Profile with Openings A and C

Figures 12a, 12b and 12c show the fluid velocity magnitudes along the two vertical sections inside the ball, having two openings. The difference between the magnitudes recorded at section 1 and 2 represents the energy gain, denoted G on the figures. G is calculated by taking the difference between the average velocity at section 1 and the average velocity at section 2. The aim of the sensitivity analysis is the find the ball design that provides the highest G possible.

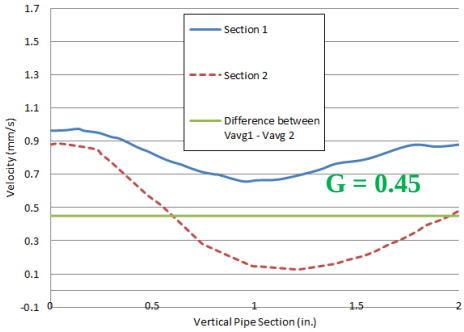

Figure 12a. Fluid Velocity Magnitudes along the Vertical Sections with Openings A and B

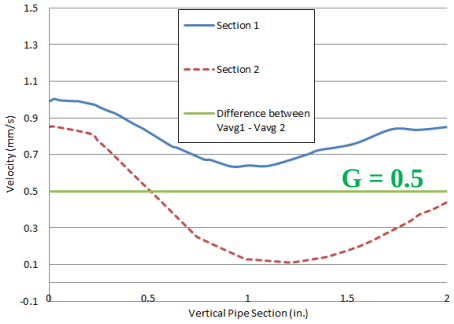

Figure 12b. Fluid Velocity Magnitudes along the Vertical Sections with Openings A and D

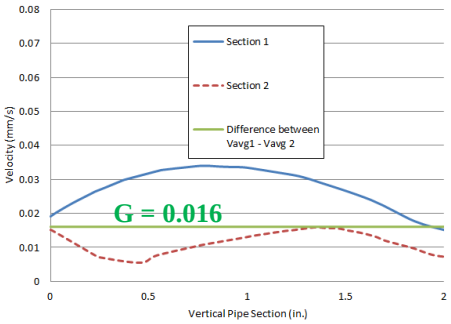

Figure 12c. Fluid Velocity Magnitudes along the Vertical Sections with Openings A and B

6.3 Numerical Simulation of Velocity Profiles when using Four Openings

To simulate the fluid flow inside the ball when using four holes, openings A, B, C and D were all opened to allow fluid flow through them. Figure 13 presents the fluid velocity propagation inside the pipe having a spherical ball with four openings. The results show how the fluid entering the ball from opening A, exits through opening B, and the fluid entering at opening C exists at opening D.

Figure 14 shows plots of fluid velocities at the created vertical sections 1 and 2. The difference between the average velocities at section 1 and the average velocities at section 2 resulted in a magnitude of 0.1 mm/s.

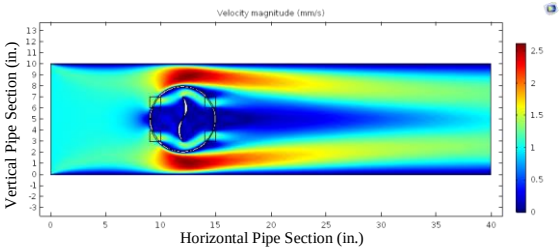

Figure 13. Velocity Propagation around and inside the Ball with Four Openings

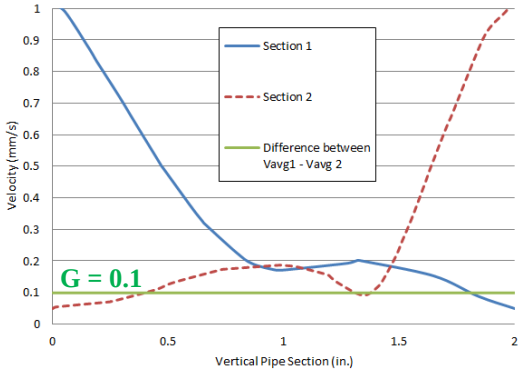

Figure 14. Fluid Velocity Magnitudes along the Vertical Sections with Four Openings

7. Discussion

The sensitivity analysis provided different energy gain results. The highest recorded G of 0.5 mm/s (half of the inlet velocity of 1 mm/s) was found when designing the ball with two openings at locations A and D. The average angular velocity ω in rad/s of the blades around the axle is calculated using the following equation:

$\omega = v/r = (0.5 \text{ mm/s}) / (25.4 \text{ mm}) = 0.02 \text{ rad/s}$

$= 0.02 \text{ rad/s} * 1 \text{ rev}/2\pi \text{ rad} = 0.2 \text{ rev/min}$

where ω represents the angular velocity, v the average fluid velocity and r the radius of curvature of the blades

The kinetic rotational energy can be found using $KE = \frac{1}{2} I \omega^2$, where KE represents the rotational kinetic energy, I the moment of inertia ($I = 4 * I_{\text{Blade, half hallow sphere}} + I_{\text{axle of rotation, cylindrical shell}} = 4 * 2/3 \text{ mr}^2 + \text{mr}^2$) and ω the angular velocity. Each blade section, having a radius of 1 in. (2.54 cm) is assumed to have a mass of 75g while the rotating axle, having a radius of 0.5 cm and length of 15.24 cm (6 in.) is assumed to have a total mass of 50 g. The kinetic rotational energy can be calculated as:

$KE = \frac{1}{2} I \omega^2$

$= \frac{1}{2} (8/3 * 75 \text{ g} * 2.54^2 \text{ cm}^2 + 50 \text{ g} * 0.5^2 \text{ cm}^2) * 0.02^2 \text{ (rad/s)}^2$

$= 0.26 \text{ g. cm}^2/\text{s}^2 = 0.026 \text{ µJ}$

Assuming a very small time period of 1 ns, the generated power from the blades in Watt is

$P = 0.026 \text{ µJ} / 0.001 \text{ µs} = 26 \text{ W}.$

Thus, to recharge the 12 V battery that will be embedded inside the ball to power the sensors, the control system and the rest of the parts, the energy gained from the blades rotation will recharge the battery at a rate of 2.2 Amp.(26W / 12V), which falls within the recommended range of battery charging practice.

8. Conclusions

The simulation results provided different energy gains from different designs of the spherical ball. This paper proved that having two openings provided the maximal velocity for the blades. The first opening should be located at the top side of the ball facing the inlet direction while the other opening should be located on the lower side of the ball facing the outlet direction. The kinetic energy and power generated from the rotation of the blades generated by the fluid flow inside the ball will be sufficient to recharge the battery embedded inside the spherical ball.

9. References

1. Chalgham, W. R., Seibi, A. C., and Boukadi, F., Simulation of Leak Noise Propagation and Detection Using COMSOL Multiphysics, *ASME Proceedings of the International Mechanical Engineering Congress & Exposition, Phoenix, Arizona, USA* (2016)
2. Chalgham, W. R., Seibi, A. C., and Lomas, M., Leak Detection and Self-Healing Pipelines Using Twin Balls Technology, *SPE Annual Technical Conference and Exhibition, Dubai, UAE* (2016)
3. Ariaratnam, S.T. and Chandrasekaran, M., Development of an Innovative Free-Swimming Device for Detection of Leaks in Oil and Gas Pipelines, *Proceedings of the 2010 ASCE Construction Research Congress "Innovation for Reshaping Construction Practices", ASCE, Banff, Alberta* (2010)
4. Bond, A., Deployment of equipment into fluid containers and conduits. *United States Patent and Trademark Office, U.S. Patent No. 6,889,703, USA* (2005)
5. Bond, A., Mergelas, B. and Jones, C., Pinpointing Leaks in Water Transmission Mains, *Proceedings of ASCE Pipelines 2004, San Diego, California, USA* (2004)
6. Calder, B., Technologies Mimic the 5 Senses to Monitor Pipelines, *Intel Free Press* (2014)
7. Carlson, M. and Henke, J., Drinking Water Pipeline Condition Assessment, *PNWS-AWWA Conference – Spokane, WA* (2013)
8. Chapman, H., Development of a Successful Internal Leak Detection and Pipeline Condition Assessment Technology for Large Diameter Pipes. *6th Annual WIOA NSW Water Industry Engineers & Operators Conference* (2012)
9. Chatzigeorgiou D., Khalifa A., Youcef-Toumi K. and Ben- Mansour R.. An in-pipe leak detection sensor: Sensing capabilities and evaluation. *ASME/IEEE International Conference on Mechatronic and Embedded Systems and Applications* (2011)
10. Dancer, B., Shenkiryk, M. and Day, S., Leak Detection Survey for a Large Diameter Transmission Main: City of Calgary, *Proceedings of the 2009 Pipelines Conference, ASCE, San Diego, CA* (2009)
11. Gernand, J. and Ojala, O., SmartBall® Inspection Report of North Beach Force Main, *Pure Americas Inc. Inspection for King County Wastewater Treatment Division, Seattle, WA* (2011)
12. James, A., The U.S. Wastes 7 Billion Gallons of Drinking Water a Day: Can Innovation Help Solve the Problem? *Climate Progress, Think Progress* (2011)
13. Khalifa A., Chatzigeorgiou D., Youcef-Toumi K., Khulief Y. and Ben-Mansour R., Quantifying acoustic and pressure sensing for in-pipe leak detection, *ASME International Mechanical Engineering Congress & Exposition* (2010)

10. Acknowledgements

The author is grateful to the University of Louisiana at Lafayette and to the advisor Dr. Seibi, who supported the simulation work and provided continuous support to this research study.